Infrared Spectra of the Novel Ge_2H_2 and Ge_2H_4 Species and the Reactive $GeH_{1,2,3}$ Intermediates in Solid Neon, Deuterium and Argon

Xuefeng Wang, Lester Andrews,* and Gary P. Kushto†

Department of Chemistry, P. O. Box 400319, University of Virginia, Charlottesville, Virginia 22904-4319

Received: January 23, 2002; In Final Form: April 15, 2002

Laser-ablated Ge atoms and H_2 molecules in excess neon and argon react during condensation to produce $GeH_{1,2,3,4}$ as identified from infrared spectra with D_2 and HD substitution, and from agreement with frequencies determined in recent gas-phase GeH and GeH_2 fluorescence spectra and DFT calculations. The novel digermanium species Ge_2H_2 and Ge_2H_4 are formed in further reactions. Identification of Ge_2H_2 with the dibridged structure and Ge_2H_4 in the trans-bent C_{2h} form is made possible by isotopic substitution and quantum chemical frequency calculations, which demonstrate the value of a close working relationship between experiment and theory. The photosensitive GeH_3^- anion is formed through electron capture by a GeH_3 radical. All four germanium deuterides are observed in pure deuterium, which shows that further GeD and GeD_2 reactions with D_2 may require activation energy.

Introduction

Germanium hydride transient species are of interest, in part, owing to their role in the growth of germanium semiconductor films in the chemical vapor decomposition process involving germane.[1−3] The most important of these, GeH_2, germylene, was produced as a vacuum-ultraviolet photolysis or discharge product of germane in matrix isolation experiments,[4,5] but the infrared absorptions were not assigned correctly. Later work identified GeH_2 from laser-induced fluorescence spectra (LIF) in the gas phase[6−9] and investigated the kinetics of germylene reactions.[10−12] The pyramidal GeH_3 radical was observed by ESR in solid krypton[13,14] and xenon,[15] infrared absorptions were attributed to GeH_3 in solid argon,[4,5] and multiphoton ionization spectra of gaseous GeH_3 have been reported.[16] The kinetics of GeH_3 radical reactions have been monitored through a transient absorption[17] at 2049.8 cm^{-1}, which is considerably higher than the reported argon matrix fundamentals.[4,5] Comparative theoretical studies of GeH_3 radicals and GeH_2 structures have been performed.[18−21] Last, but not least, the diatomic transient GeH and GeD radicals have been thoroughly investigated under high-resolution conditions.[22,23]

The unsaturated digermanium species have been explored by theoretical calculations and found to have unusual structures, unlike their hydrocarbon analogues. The ground state of Ge_2H_2 is a C_{2v} "butterfly" structure,[24−27] like Si_2H_2, and Ge_2H_4 has a nonplanar C_{2h} geometry, like Si_2H_4.[27−31] However, the saturated Ge_2H_6 molecule has the ethane structure.[27,30] Finally, the Ge_2H_4 species has been proposed as a reaction product in the decomposition of GeH_4.[32]

We report here a combined neon, deuterium, and argon matrix infrared and density functional theoretical investigation of the above germanium hydride transient species. The new matrix identifications are greatly facilitated by recent gas-phase measurements of GeH and GeH_2 fundamentals,[6−9,22,23] by quantum chemical calculations,[25] and by neon matrix experiments where diffusion and dimerization of small transients during 3.5 K deposition are favorable reactions. This work reassigns the matrix infrared spectra of $GeH_{1,2,3}$ and provides the first experimental evidence for the unsaturated Ge_2H_2 and Ge_2H_4 species.

Experimental and Theoretical Methods

Laser-ablated germanium (Alfa, 99.999%) atoms were reacted with H_2, D_2, and HD (0.2−10%) in excess argon and neon and with pure deuterium during condensation at 3.5 K using a Sumitomo Heavy Industries RDK-205D Cryocooler and methods described previously.[33,34] Infrared spectra were recorded, samples were annealed and irradiated, and more spectra were recorded. Complementary density functional theory DFT calculations were performed using the Gaussian 98 program, BPW91 and B3LYP density functionals, 6-311++G(d,p) basis, and SDD pseudopotential.[35−39] Geometries were fully optimized, and the vibrational frequencies were computed analytically from second derivatives.

Results

Infrared spectra from neon, deuterium, and argon matrix experiments with Ge and H_2 and DFT calculations on expected products will be presented. Table 1 lists the observed product absorptions.

Neon Matrix. Infrared spectra of solid neon films containing reaction products of laser-ablated Ge and 5% H_2 are shown in Figure 1 and D_2 counterparts in Figure 2. The strongest absorption is at 1859.8 (1340.9) cm^{-1} for H_2 (D_2) reactions. The weak 1925.5 cm^{-1} absorption is due to GeCO, recently identified at 1918.9 cm^{-1} in solid argon.[40] The weak 1757 cm^{-1} band that grows on 8 K annealing is unshifted with HD and D_2. A very weak GeO absorption[41,42] appears at 977.0 cm^{-1} just above new bands at 972.2, 921.3, and 903.3 cm^{-1}. Note the much larger yield of GeH_4 than GeD_4 at 2114.3 (1522.0) cm^{-1};[43] annealing doubles the latter absorptions and sharpens the former bands into doublets 1862.4, 1859.8 (1342.6, 1337.3) cm^{-1}. The HD experiment gives slightly different sharp bands

* Author for correspondence: lsa@virginia.edu.
† Present address: Optical Sciences Branch, United States Naval Research Laboratory, Washington, DC 20375.

10.1021/jp020219v CCC: $22.00
Published on Web 05/24/2002

TABLE 1: Infrared Absorptions (cm^{-1}) Observed for Reactions of Laser-Ablated Germanium Atoms with Hydrogen and Deuterium in Solid Matrices

matrix	H_2	D_2	identification
Ne	1834.2	1321.2	GeH, GeD
	1832.2	1319.5	GeH, GeD site
D_2		1316.1	GeD site
		1313.6	GeD
Ar	1813.5	1305.3	GeH, GeD
		1303.8	GeH, GeD site
Ne	1867.6		GeH_2 site
	1862.5	1342.6	GeH_2, GeD_2
	1860.4	1337.3	GeH_2, GeD_2
	1855.7		GeH_2 (agg)
	921.5	660.2	GeH_2, GeD_2
	903.5	648.5	GeH_2, GeD_2 (agg)
D_2		1338.4	GeD_2
		1335.7	site
		1332.7	GeD_2
		1330.4	site
		646.5	GeD_2
Ar	1839.2	1325.4	GeH_2, GeD_2
	1835.3	1322.0	GeH_2, GeD_2 (agg)
	1830.5		GeH_2, GeD_2 (agg)
	913.6	654.4	GeH_2, GeD_2
Ne	2089.4	1504.7	GeH_3, GeD_3 (ν_3)
	857.2	611.3	GeH_3, GeD_3 (ν_4)
	667.8	489.5	GeH_3, GeD_3 (ν_2)
D_2		1500.9	GeD_3
		610.6	GeD_3
		488.0	GeD_3
Ar	2074.1	1496.5	GeH_3, GeD_3
	852.4		GeH_3, GeD_3
	667.0		GeH_3
Ne	2114.3	1522.0	GeH_4, GeD_4
	822.3	594.5	GeH_4, GeD_4
D_2		1516.8	GeD_4
		590.9	GeD_4
Ar	2106.3	1516	GeH_4, GeD_4 site
	2098.7[a]	1513.2[a]	GeH_4, GeD_4
	814.5[a]	591.0[a]	GeH_4, GeD_4
Ne	1352.3		Ge_2H_2
	972.2	715.1	Ge_2H_2, Ge_2D_2
Ar	1340.0		Ge_2H_2
	964.3	709.3	Ge_2H_2, Ge_2D_2
Ne	(2053)	1479.0	Ge_2H_4, Ge_2D_4
	(2035)	1465.7	Ge_2H_4, Ge_2D_4
	789.1	569.5	Ge_2H_4, Ge_2D_4
Ar		1476	Ge_2D_4
	787	568	Ge_2H_4, Ge_2D_4
Ne	881.6	631.5	Ge_2H_6, Ge_2D_6
	752.8	542.5	Ge_2H_6, Ge_2D_6
D_2		542.0	Ge_2D_6
Ne	1700	1234	GeH_3^-, GeD_3^- (ν_3, e)
	1670	1208	GeH_2^-, GeD_2^-
D_2		1219.9	GeD_3^-
		1202.4	GeD_2^-

[a] Band positions appear subject to effects of aggregation; compare ref 4.

at 1858.4 and 1338.4 cm^{-1}. Broad-band photolysis increases 2053, 2035 (1479.0, 1465.7) cm^{-1} bands, destroys 1704, 1670 (1234, 1208) cm^{-1} peaks, and decreases 972.2 (715.1) cm^{-1} features. Figure 3 shows the evolution of site structure on the major product band and the relative intensities of different product species using 1% and 0.2% H_2 with different laser energies. Under more dilute 0.2% H_2 conditions, only the 1670 cm^{-1} intermediate band is observed, and $\lambda > 380$ nm irradiation destroys the 1670 (1208) cm^{-1} bands. The 972.2 (715.1) cm^{-1} absorptions are compared in Figure 4 with HD and mixed $H_2 + D_2$ product spectra.

Deuterium Matrix. Infrared spectra of pure D_2 co-deposited with Ge atoms at 3.5 K are illustrated in Figure 5. Note weak

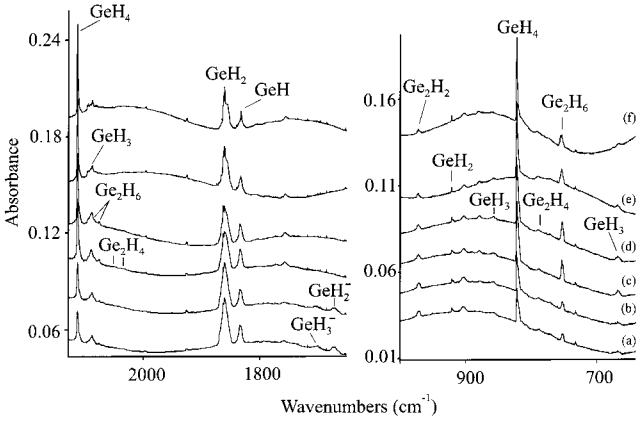

Figure 1. Infrared spectra of neon matrix formed by co-depositing hydrogen and laser-ablated germanium: (a) 5% H_2 in neon deposited for 60 min at 3.5 K, (b) after annealing to 7 K, (c) after $\lambda > 240$ nm photolysis for 15 min, (d) after annealing to 8 K, (e) after annealing to 10 K, and (f) after annealing to 12 K.

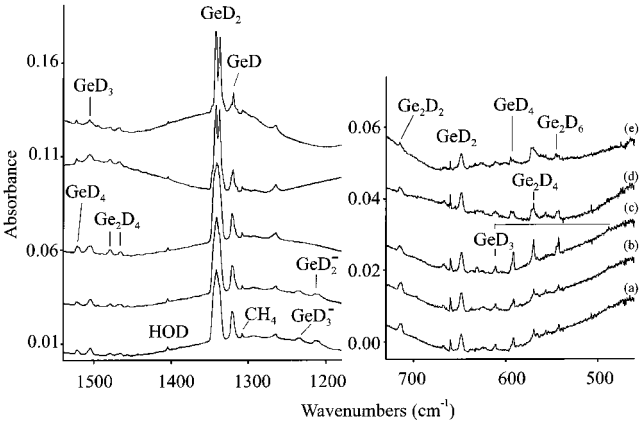

Figure 2. Infrared spectra of neon matrix formed by co-depositing deuterium and laser-ablated germanium: (a) 5% D_2 in neon deposited for 60 min at 3.5 K, (b) after annealing to 7 K, (c) after $\lambda > 240$ nm photolysis for 15 min, (d) after annealing to 8 K, (e) after annealing to 10 K, and (f) after annealing to 12 K.

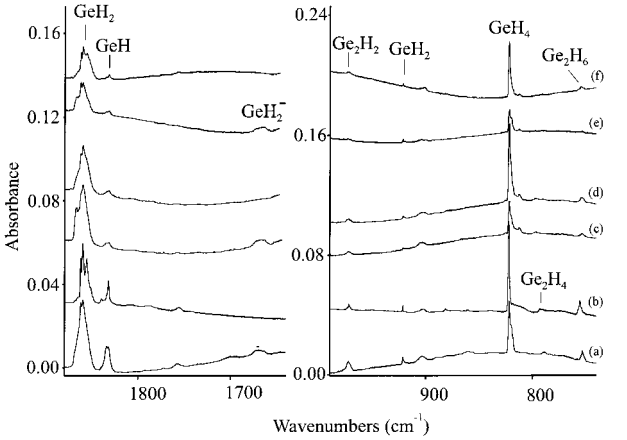

Figure 3. Infrared spectra of neon matrix formed by co-depositing hydrogen and laser-ablated germanium: (a) 1% H_2 in neon deposited for 60 min, (b) after annealing to 13 K, (c) 1% H_2 in neon with reduced laser energy deposited for 60 min, (d) after annealing to 9 K, (e) 0.2% H_2 in neon with reduced laser energy deposited for 60 min, and (f) after annealing to 11 K.

GeD_4 bands at 1516.8 and 590.9 cm^{-1} on deposition that increase on ultraviolet photolysis and important new absorptions at 1500.9, 1338.4, 1332.7, 1313.6, 1219.9, and 1202.4 cm^{-1} that show different photolysis and annealing behaviors. Another

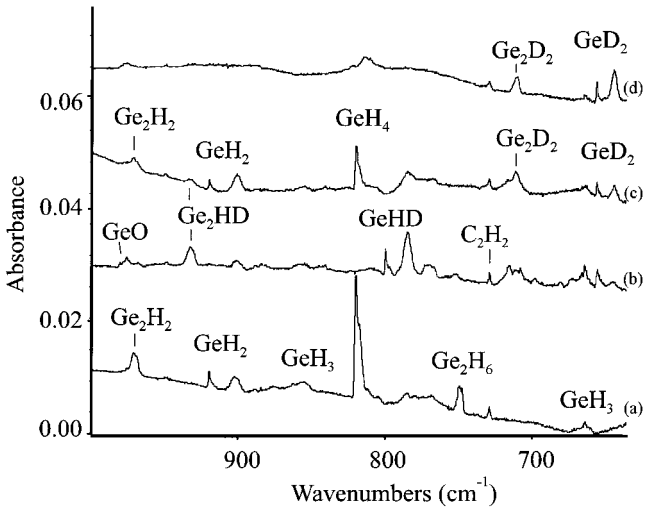

Figure 4. Infrared spectra of germanium−hydrogen reaction products: (a) 5% H_2 in neon, (b) 6% HD in neon, (c) 3% H_2 + 3% D_2 in neon, and (d) 5% D_2 in neon.

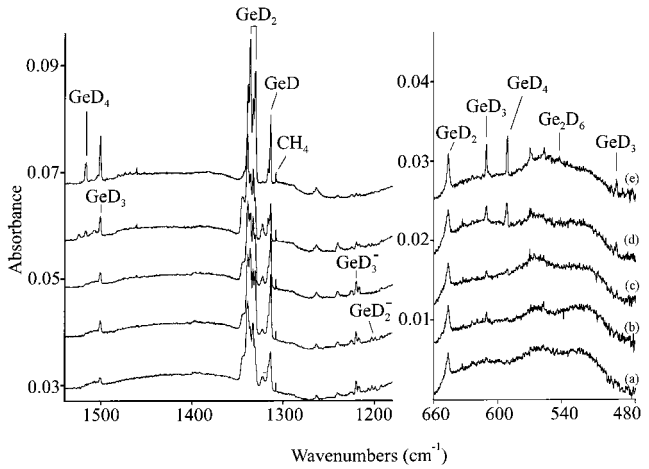

Figure 5. Infrared spectra of pure deuterium co-deposited with laser-ablated Ge atoms: (a) 25 min deposit, (b) after annealing to 7 K, (c) after $\lambda > 380$ nm photolysis for 15 min, (d) after 240−380 nm photolysis for 15 min, and (e) after annealing to 8 K.

experiment with higher laser energy gave increased product band intensities except for the latter photosensitive bands, which were not observed.

Argon Matrix. Infrared spectra for Ge and 2% H_2 reaction products in solid argon at 7 K are shown in Figure 6 where the product distribution is different from that in neon owing to the faster condensation rate of argon under the condition of these experiments. A weak GeO band is observed at 975 cm^{-1}, and weak HO_2 bands appear at 1389 and 1101 cm^{-1} on annealing and attest the production of H atoms.[44] The broad 2106.3 cm^{-1} GeH_4 band dominates the sharp 2098.8 cm^{-1} absorption on deposition, but annealing favors the latter, while the GeH_4 band at 816.8 cm^{-1} shifts to 814.3 cm^{-1}, and a weak 964.3 cm^{-1} absorption increases. Likewise satellite features at 1889.2, 1868.2, and 1848.1 cm^{-1} give way on annealing to the dominant 1839.2 and 1813.5 cm^{-1} bands. The HD experiment gives a slightly different 1835.8 cm^{-1} former band but the same 1813.5 cm^{-1} latter band. Argon matrix experiments using a 3.5 K substrate and 10% H_2 trap a smaller yield of the same product bands owing to the faster condensation rate, but these include a new 1675 cm^{-1} absorption. At the higher H_2 concentration, the 748.5 cm^{-1} band grows more on annealing and the 964.3 cm^{-1} band grows less, relative to the 1839.2 cm^{-1} feature. Table

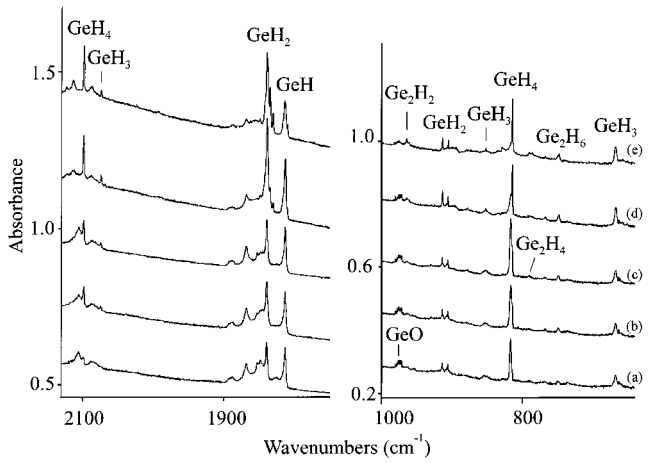

Figure 6. Infrared spectra of argon matrix formed by co-depositing hydrogen and laser-ablated germanium: (a) 2% H_2 in argon deposited for 60 min at 7 K, (b) after annealing to 18 K, (c) after $\lambda > 240$ nm photolysis for 15 min, (d) after annealing to 28 K, and (e) after annealing to 38 K.

1 collects the H_2 and D_2 reaction product bands for the three different matrix environments.

Calculations. DFT calculations were done for the subject species using B3LYP and BPW91 functionals to predict a consistent set of germanium hydride product vibrational frequencies for H, D, and mixed isotopic molecules to aid in making vibrational assignments. Table 2 lists the H isotopic frequencies and Table 3 gives the D isotopic counterparts.

Our B3LYP calculations of the novel Ge_2H_2 and Ge_2H_4 structures are in excellent agreement with previous results. In the case of Ge_2H_2, MP2 calculations find slightly shorter bonds but nearly the same angles, and CISD predicts Ge−H bonds 0.03 Å shorter, a Ge−Ge bond 0.08 Å shorter, nearly the same angles, and slightly higher frequencies.[25,26] In the case of Ge_2H_4, SCF finds a 0.1 Å shorter Ge−Ge bond, 0.03 Å shorter Ge−H bonds, and similar angles, and other calculations are in these ranges.[30] Analogous B3LYP calculations using the larger 6-31++G(2d,2p) basis set gave slightly longer Ge−H but shorter Ge−Ge bonds for Ge_2H_2 and both shorter bonds for Ge_2H_4 again with similar angles.[27]

Discussion

The new product absorptions will be assigned to germanium hydride species on the basis of isotopic substitution, comparison of neon, argon, and deuterium matrix results, and agreement with DFT frequency calculations.

GeH. The neon matrix absorptions at 1834.2, 1832.2 (1321.2, 1319.5) cm^{-1} can be assigned to the GeH (GeD) diatomics (1.388 H/D ratio) on the basis of the agreement with the gas-phase fundamentals at 1833.8 and 1319.8 cm^{-1}, respectively, from electronic band spacings.[22,23] The neon matrix bands shift to 1813.5 and 1305.3 cm^{-1} in solid argon, which are in line with other such comparisons.[46] A sharp band at 1313.6 cm^{-1} in pure deuterium (Figure 5) is also assigned to GeD. Smith and Guillory[4] assigned the 1305 cm^{-1} GeD band in solid argon but misassigned the 1813 cm^{-1} absorption to GeH_3. Our B3LYP and BPW91 calculations (Table 2) and others come in slightly low for the GeH fundamental, but CCSD(T) calculations give higher frequency values.[47,48]

GeH_2. The strongest product absorptions at 1859.8 cm^{-1} with H_2 and at 1340.9 cm^{-1} with D_2 in neon (Figures 1 and 2) are candidates for GeH_2 and GeD_2. Annealing sharpens these absorptions to 1862.5, 1860.4, and 1855.7 cm^{-1} and a resolved

TABLE 2: Frequencies (cm^{-1}), Infrared Intensities (km/mol), Bond Lengths, and Angles Calculated at the DFT/6-311++G(d,p)/SDD Level for Germanium Hydrides

	B3LYP[a]	BPW91[a]	other	experimental
GeH	1818.0 (533)	1772.4 (476)	1844	[1833.8, 1.587 Å][c]
$^2\Pi$	1.626 Å	1.642 Å	1.608 Å[b]	1813.5, 1833.8[d,e]
GeH_2	1851.5 (a_1, 450)	1800.5 (b_1, 460)	1840, 913, 1840[f]	[1856, 916, 1.588 Å][f]
$^1A_1$	1848.4 (b_1, 514)	1795.4 (a_1, 414)	1.613 Å, 93.2°	1839.2, 1862.4[d,e]
(C_{2v})	936.9 (a_1, 76)	898.6 (a_1, 63)	2059, 1036, 2057[g]	
	1.617 Å, 90.7°	1.624 Å, 89.9°	1.575 Å, 93.0°	
GeH_3	2081.7 (e, 249 × 2)	2031.5 (e, 224 × 2)	2227[h]	[663 (10)][i]
$^2A_1$	2051.9 (a_1, 23)	1986.6 (a_1, 22)	2212	2074.2, 852.4, 667.6[d]
(C_{3v})	847.8 (e, 62 × 2)	820.3 (e, 52 × 2)	937	2089.4, 857.2, 667.8[e]
	718.9 (a_1, 76)	686.3 (a_1, 58)	782	
	1.554 Å, 110.5°	1.566 Å, 110.5°	1.539 Å, 110.8°	
GeH_4	2139.3 (a_1, 0)	2070.3 (a_1, 0)	2279 (0)[g]	[2114, 819, 1.516 Å][j]
$^1A_1$	2118.3 (t_2, 205 × 3)	2067.1 (t_2, 187 × 3)	2259 (122)	2098.7, 814.5[d]
(T_d)	912.0 (e, 0)	884.3 (e, 0)	1009 (0)	2114.3, 822.3[e]
	821.7 (t_2, 136 × 3)	785.6 (t_2, 107 × 3)	920 (127)	
	1.547 Å	1.558 Å	1.535 Å	
Ge_2H_2	1415.5 (a_1, 36)	1389.9 (a_1, 32)	1534 (12)[l]	
$^1A_1$	1332.6 (b_1, 100)	1326.8 (b_1, 84)	1446 (51)	
(C_{2v})	1004.2 (b_2, 342)	1019.7 (b_2, 302)	1054 (469)	964.3, 972.2[d,e]
	874.7 (a_2, 0)	930.1 (a_2, 0)	931 (0)	
	815.7 (a_1, 83)	787.9 (a_1, 67)	863 (42)	
	265.8 (a_1, 1)	262.3 (a_1, 1)	304 (0)	
	Ge−H: 1.802 Å	Ge−H: 1.813	Ge−H: 1.771	
	Ge−Ge: 2.459 Å	Ge−Ge: 2.470	Ge−Ge: 2.377	
	Ge−H−Ge: 86.1°	Ge−H−Ge: 86.1°	HGeGeH: 105.5°	
	H−Ge−H: 71.4°	H−Ge−H: 71.1°		
	HGeGeH: 105.9°			
Ge_2H_4	2057.9 (a_u, 443)	2002.0 (a_u, 367)		(2053), (2035)
^1A_g	2038.4 (b_g, 0)	1982.1 (b_g, 0)		789[e]
(C_{2h})	2033.0 (b_u, 430)	1968.5 (b_u, 381)		
	2031.4 (a_g, 0)	1963.9 (a_g, 0)		
	879.2 (b_u, 240)	851.4 (b_u, 209)		
	Ge−H: 1.562 Å	Ge−H: 1.576	Ge−H: 1.528[k]	
	Ge−Ge: 2.372 Å	Ge−Ge: 2.373	Ge−Ge: 2.270	
	H−Ge−H: 105.8°	H−Ge−H: 106.0°	H−Ge−H: 109.8°	
	Ge−Ge−H: 114.6°	Ge−Ge−H: 114.5°	Ge−Ge−H_2: 145.4	
Ge_2H_6	2102.4 (e_u, 381 × 2)	2051.0 (e_u, 343 × 2)		[2093, 2077, 879, 756][j]
$^1A_{1g}$	2097.4, (a_{2u}, 245)	2034.1 (a_{2u}, 244)		878.2, 748.7[d]
(D_{3d})	878.6 (e_u, 86 × 2)	849.5 (e_u, 69 × 2)		881.6, 752.8[e]
	750.8 (a_{2u}, 610)	722.1 (a_{2u}, 524)		
	Ge−H: 1.550 Å	Ge−H: 1.562	Ge−H: 1.531[k]	
	Ge−Ge: 2.484 Å	Ge−Ge: 2.487	Ge−Ge: 2.477	
	H−Ge−H: 108.5°	H−Ge−H: 108.4°	H−Ge−H: 108.7°	
GeH^-	1537.2 (1308)			
$^1\Pi$	Ge−H: 1.685 Å			
($C_{\infty h}$)				
GeH_2^-	1587.1 (a_1, 1145)	1550.6 (a_1, 1045)		1670[e]
$^2B_1$	1576.3 (b_2, 1318)	1550.6 (b_2, 1184)		
(C_{2v})	861.5 (a_1, 81)	824.1 (a_1, 67)		
	Ge−H: 1.670 Å	Ge−H: 1.685 Å		
	H−Ge−H: 90.5°	H−Ge−H: 89.9°		
GeH_3^-	1650.9 (a_1, 823)	1605.5 (e, 1074 × 2)		1700[e]
$^1A_1$	1638.3 (e, 1193 × 2)	1600.2 (a_1, 780)		
(C_{3v})	877.3 (e, 34 × 2)	842.6 (e, 28 × 2)		
	831.6 (a_1, 112)	799.2 (a_1, 92)		
	Ge−H: 1.652 Å	Ge−H: 1.668 Å	Ge−H: 1.623[m]	
	H−Ge−H: 92.2°	H−Ge−H: 91.5°	H−Ge−H: 93.2°	

[a] This work, infrared intensities in parentheses. [b] CCSD(T)/ECP/SDB, ref 48. [c] Gas phase, ref 23. [d] This work: argon matrix, cm^{-1}. [e] This work: neon matrix, cm^{-1}. [f] Gas phase, refs 8 and 9. [g] DHF, ref 49. [h] Reference 20. [i] Reference 16. [j] Gas phase, refs 43 and 45. [k] Reference 30. [l] Reference 25. [m] Reference 54.

doublet at 1342.6, 1337.3 cm^{-1}. The 1862.5 cm^{-1} band is much sharper than the 1860.4, 1855.7 cm^{-1} absorptions; so they are probably due to different matrix sites. The blue site at 1867.6 cm^{-1} (Figure 3) disappears first on annealing and photolysis while GeH_4 increases; therefore, it is presumed to be due to a $(H_2)GeH_2$ complex. The sharp 1862.5 and 1860.4 cm^{-1} bands appear to track with the sharp 921.5 cm^{-1} feature, whereas the broader 1855.7 cm^{-1} peak and red shoulders track with the broad 903.5 cm^{-1} band, which shifts to 901.4 cm^{-1} on annealing.

The gas-phase fluorescence spectra of GeH_2 and GeD_2 revealed symmetric vibrational fundamentals at 1856, 916, and 1335, 657 cm^{-1}, respectively.[8,9] Supporting B3LYP frequency calculations (Table 2) and other calculations[8,49] predict the antisymmetric and symmetric stretching fundamentals for GeH_2 to be within a few cm^{-1} of each other and the former slightly more intense. Hence, the sharp resolved 1342.6, 1337.3 cm^{-1} neon matrix bands are appropriate for ν_3 (b_1) and ν_1 (a_1) of GeD_2, but matrix sites contribute to the band contour for

TABLE 3. Important Frequencies (cm^{-1}) Calculated at the DFT/6-311++G(d,p)/SDD Level for Germanium Deuterides[a]

	B3LYP	BPW91
GeD	1294.9	1262.4
GeD_2	1318.2	1282.4
	1316.6	1278.5
	667.4	639.9
GeD_3	1485.5	1449.8
	1453.4	1407.2
	604.2	584.7
	517.7	494.5
GeD_4	1513.3	1474.0
	1510.4	1464.5
	645.1	625.6
	591.7	565.7
Ge_2D_2	1003.1	985.5
	946.8	942.6
	717.3	728.4
	621.9	661.3
	586.7	566.6
	264.5	260.9
Ge_2D_4	1469.2	1428.4
	1454.8	1410.4
	1445.6	1398.9
	1445.1	1398.4
	627.5	607.6
Ge_2D_6	1499.8	1463.0
	1486.5	1441.6
	625.6	604.9
	540.7	520.0
GeD^-	1094.9	
GeD_2^-	1129.9	1104.4
	1122.8	1104.1
	613.7	587.0
GeD_3^-	1173.9	1143.6
	1167.0	1138.1
	622.9	598.2
	596.9	573.5

[a] Frequencies in same order and relative intensities as hydrogen counterparts in Table 2.

GeH_2 and specific modes are not resolved. Our HD experiment gave single sharp bands at 1857.2 and 1338.3 cm^{-1} in each region, although a very sharp 1858.9 cm^{-1} satellite evolved with the former band on annealing. The ν_1 mode of GeD_2 in solid neon is within 2 cm^{-1} of the gas-phase value.[9] These bands show H/D ratios 1860.4/1342.6 = 1.386 that are typical of Ge−H stretching vibrations. Germane itself reveals the 2114.3/1522.0 = 1.389 ratio. In addition, we observe the isolated GeH_2 and GeD_2 bending modes at 921.5 and 660.2 cm^{-1}, which are blue shifted 5 and 3 cm^{-1} by the neon matrix, and our GeHD value is 802.2 cm^{-1}. We note that the bending mode is sufficiently low that the overtone does not reach the stretching mode region. Finally the broader red-shifted features are due to GeH_2 aggregated with other species in the neon matrix.

Our 1839.2 and 1325.4 cm^{-1} argon matrix bands appear to be counterparts of the above neon matrix absorptions (H/D = 1.388). Bands in the latter region (1329 cm^{-1}) were assigned by Smith and Guillory to GeD_2, but the 1887, 1864 cm^{-1} and 1890, 1870 cm^{-1} bands assigned to GeH_2 in solid argon[4,5] are not compatible with the neon matrix spectrum (nor are the 1887 and 1329 cm^{-1} bands[4] compatible with each other, as their 1.420 ratio is too high for a Ge−H mode). The former bands are probably due to an aggregate species, possibly a GeH_2 complex with H_2, but we cannot be certain. However, the 1839 cm^{-1} argon matrix band first assigned[4] to GeH_3 is here reassigned to GeH_2 whereas the 1325 cm^{-1} band is correctly assigned to GeD_2.

The sharp 1338.4 and 1332.7 cm^{-1} bands in pure deuterium are counterparts to the above GeD_2 absorptions. Note the survival of GeD_2 in pure D_2 and the trend of deuterium matrix absorptions appearing between neon and argon matrix values.

The present argon matrix 1839.2 and 913.6 cm^{-1} assignments to GeH_2 may be compared with the spectrum of GeH_2 in the H_2O-GeH_2 complex for which Ge−H stretching modes at 1813.6 and 1777.2 cm^{-1} and bending mode at 897.8 cm^{-1} were identified.[50] Although the symmetric Ge−H stretching mode was complicated by a Fermi resonance with the bending mode overtone, it appears that the two Ge−H bands are nonequivalent in the H_2O-GeH_2 complex.

GeH_3. DFT calculations (Table 2) using two functionals predict the strongest GeH_3 fundamental, the ν_3 (e) mode, 36 cm^{-1} below the strongest GeH_4 absorption. Previous HF calculations find a 13 cm^{-1} difference.[20] Hence, the new 2089.4 and 1504.7 cm^{-1} neon matrix absorptions, 25 and 17 cm^{-1}, respectively, below GeH_4 and GeD_4, are appropriate for GeH_3 and GeD_3. In pure deuterium, a stronger new 1500.9 cm^{-1} absorption is 16.0 cm^{-1} below GeD_4 at 1516.9 cm^{-1}. Sharp, new argon matrix counterparts were observed slightly lower at 2074.1 and 1496.5 cm^{-1}. In addition, the GeH_4 discharge work[5] shows a product band near 2073 cm^{-1} that can now be assigned to GeH_3. This new assignment for ν_3 (e) of GeH_3 is compatible with diode laser monitoring of GeH_3 radicals at 2049.8 cm^{-1}, but not with earlier matrix assignments[4,5] of a band near 1839 cm^{-1}, which is assigned above to GeH_2.

Support is also found for this new GeH_3 assignment in the HD experiment, which gives new bands for GeH_2D and $GeHD_2$. Three bands are observed at 1505, 1479, and 2071 cm^{-1} for $GeHD_2$ and at 2088, 2062, and 1493 cm^{-1} for GeH_2D, which agree with the separations predicted by our DFT calculations.

In addition, the ν_4 and ν_2 fundamentals for the GeH_3 radical are observed here at 857.2 and 667.8 cm^{-1} in solid neon with deuterium counterparts in solid neon and deuterium (Table 1). The matrix ν_2 frequency is in excellent agreement with recent MPI work.[16] These assignments are substantiated by DFT frequency calculations (Table 2).

GeH_4 and Ge_2H_6. The observation of germane in these experiments supports the above assignments, as further reactions of $GeH_{1,2,3}$ should produce GeH_4. The present argon matrix experiments produce the same sharp GeH_4 and GeD_4 absorption observed with the authentic material, but the extra higher frequency absorption[45,50] is much weaker here. This latter peak might be due to a germane aggregate species. In the pure deuterium experiment, the GeD_4 absorption at 1516.9 cm^{-1} is much weaker than GeD_3 at 1500.9 cm^{-1} on sample deposition, but $\lambda > 240$ nm photolysis reduces GeD_3 and increases GeD_4 and Ge_2D_6.

Likewise, the observation of digermane is also expected in these reactions from the dimerization of GeH_3. The two strong (ν_6 and ν_8) bands of Ge_2H_6 (Ge_2D_6) are observed here.[4,45] The strong Ge−H stretching modes of digermane are difficult to resolve, but the weak 2096.5 and 2077.0 cm^{-1} bands are probably due to Ge_2H_6. In our pure deuterium experiment, Ge_2D_6 increases on photolysis at the expense of GeD_3, and a sharp 1510.4 cm^{-1} band appears. The 1510.4 cm^{-1} band is probably due to Ge_2D_6 in solid deuterium.

Ge_2H_2. The neon matrix experiments reveal a new band at 972.2 cm^{-1}, which decreases slightly on $\lambda > 240$ nm irradiation and annealing. In contrast, the Ge_2H_6 absorptions double on photolysis and quadruple on annealing. The 972.2 cm^{-1} absorption increases relative to the GeH_2 bands on increasing the relative Ge/H_2 reagent ratio through the use of higher laser energy (Figure 3). This band shifts to 715.1 cm^{-1} with D_2 and gives a 1.360 ratio, which is lower (more anharmonic) than

found for terminal Ge−H stretching modes. In addition, one HD counterpart was observed at 934.5 cm^{-1}, substantially above the median band position. For an uncoupled symmetric mode, like the bending mode of GeH_2, the GeHD value (802.2 cm^{-1}) is just above the mean of GeH_2 and GeD_2 values (921.5 and 660.2 cm^{-1} average to 790.0 cm^{-1}). The single unique HD counterpart and the observation of no new bands with the $H_2 + D_2$ mixture demonstrate that a single H_2 molecule is involved here. The 972.2 cm^{-1} band, then, is due to the antisymmetric motion of two H atoms where symmetry lowering on HD substitution results in a different mode (the strongest band of Ge_2HD has more H than D motion) since the Ge_2HD counterpart at 934.5 cm^{-1} is substantially higher than the $Ge_2H_2-Ge_2D_2$ median (843.6 cm^{-1}).

This new 972.2 cm^{-1} absorption is in the region predicted earlier[25] for the strongest antisymmetric (b_2) absorption of C_{2v} "butterfly" dibridged Ge_2H_2. Our B3LYP calculations give 1004.2, 950.9, and 717.3 cm^{-1} for this strong mode of Ge_2H_2, Ge_2HD, and Ge_2D_2, respectively, and the solid neon bands at 972.2, 934.5, and 715.1 cm^{-1} fit this pattern very well except for the lack of anharmonicity in the calculated frequencies. This match of an unusual isotopic frequency pattern confirms the matrix identification of Ge_2H_2, which is isostructural with Si_2H_2, and both are nonplanar dibridged analogues of linear HC-CH.[24,25,51,52] Other modes of Ge_2H_2 are much weaker: although DFT predicts the b_1 stretching mode to be 29% as intense, the higher level calculations find it to be only 10% as strong.[25] A 1352.3 cm^{-1} band 7% as strong as 972.2 cm^{-1} follows on annealing and photolysis and exhibits an identical 1.1 cm^{-1} higher splitting on 9 K annealing. The 1352.3 cm^{-1} absorption is assigned to the antisymmetric (b_1) mode calculated near 1330 cm^{-1} by DFT and 1420 cm^{-1} by CCSD;[25] the much weaker Ge_2D_2 counterpart is not observed. Our DFT structure for Ge_2H_2 is illustrated below.

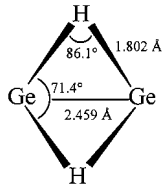

The argon matrix b_2 mode isotopic counterparts were observed at 964.3, 927.8, and 709.3 cm^{-1}. These bands increase more on annealing in solid argon as higher temperatures can be attained, and they exhibit matching satellites 3.4 cm^{-1} lower. The 964.3 cm^{-1} band increases at the expense of GeH_2 on final 38 K annealing (Figure 6). In addition, the 964.3 cm^{-1} band grows more on annealing than Ge_2H_6 in 2% H_2 argon matrix experiments, but Ge_2H_6 increases substantially more than Ge_2H_2 on annealing with 10% H_2 in argon. Finally, Ge_2D_2 was not observed in pure deuterium.

Smith and Guillory[4] show a weak absorption near 960 cm^{-1} in a Ge_2H_6 experiment before photolysis; this band is more than an order of magnitude weaker than the 878 cm^{-1} Ge_2H_6 band. Hence, their 964 cm^{-1} product band in GeH_4 experiments, which is comparable to the 878 cm^{-1} band in intensity, is probably due to Ge_2H_2, as we assign above, and not to Ge_2H_6. We note that Ge_2H_6 vapor has no absorption near 960 cm^{-1}.[45]

Ge_2H_4. Two new bands appear at 1479.0 and 1465.5 cm^{-1} below GeD_3 in neon at 1504.7 cm^{-1}: these bands increase substantially on broad-band photolysis (Figure 2). Very weak 2053 and 2035 cm^{-1} bands with H_2 exhibit similar behavior: these weak bands exhibit appropriate 1.388, 1.389 H/D ratios with the stronger D_2 products. B3LYP calculations (Table S3) predict Ge_2D_4 to have two strong absorptions 17 and 40 cm^{-1} below the strongest GeD_3 radical absorptions, and the 1479.0 and 1465.5 cm^{-1} absorptions 26 and 39 cm^{-1} lower fit nicely. Our HD experiment gives a weak 1471 cm^{-1} absorption intermediate between the above bands, as is predicted by calculations. We would be more confident about assigning these bands to Ge_2H_4 and Ge_2D_4 if stronger hydrogen counterparts were observed. However, it is probable that Ge_2D_4 is made in much higher yield in these experiments than Ge_2H_4. The GeH_4 band is 10 times stronger than the GeD_4 band in Figures 1 and 2, and accounting for the relative infrared intensities, the yield of GeH_4 is 5 times greater. This shows that more GeH_2 reacts with H_2 during condensation in neon and suggests that less GeH_2 would be available for dimerization. A strong 569.5 cm^{-1} band with D_2 in neon tracks with the 1479.0, 1465.5 cm^{-1} doublet on photolysis and annealing. The weaker H_2 counterpart at 789.1 cm^{-1} defines a 1.386 H/D ratio, which is appropriate for a bending mode. Our DFT calculation predicts a very strong bending mode for Ge_2H_4 at 879.3 cm^{-1}, which is slightly higher than the observed band, but reasonable for this unusual molecule. The HD experiment gives a single counterpart at 703.0 cm^{-1}.

In solid argon, the product yield was very low and annealing to 35 K produced new 1476 and 568 cm^{-1} bands, which are argon matrix counterparts of Ge_2D_4. Only the 787 cm^{-1} bending mode was observed in argon for Ge_2H_4.

Accordingly, the above absorptions are assigned to Ge_2H_4 and Ge_2D_4, which are novel nonplanar analogues of ethylene.[27−31] The only previously observed Ge═Ge moiety is the substituted Ge_2R_4 species, which has the trans-folded framework.[53]

GeH_3^- and GeH_2^-. Two bands at 1700 and 1670 cm^{-1} are unique in that broadband irradiation eliminates and further annealing does not restore them. Furthermore, a similar 5% H_2 experiment doped with 0.1% CCl_4 gave the other product bands with 50−70% of their former absorbances, but the 1700 and 1670 cm^{-1} bands were not observed. Such treatment has been found to prevent product anion formation owing to preferential electron capture by CCl_4.[54−56] Hence, the latter absorptions are appropriate for anions, and DFT calculations were performed for possible anion species. Table 2 shows that GeH_3^- and GeH_2^- absorptions fall in this region, and the above bands must be considered accordingly.

These absorptions shift to 1234 and 1208 cm^{-1} with D_2 in neon, giving 1.378 and 1.382 H/D frequency ratios, which is appropriate for a terminal Ge−H stretching frequency. Broad-band photolysis destroyed both of these absorptions, but in a second experiment irradiation with a $\lambda > 380$ nm filter destroyed the 1208 cm^{-1} band without affecting the 1234 cm^{-1} absorption; the 1670 cm^{-1} band was also destroyed by $\lambda > 380$ nm but not affected by $\lambda > 470$ nm radiation, whereas the 1700 cm^{-1} band was not affected at $\lambda > 380$ nm but diminished at $\lambda > 290$ nm. It is clear that the lower band is more photosensitive than the upper band. The pure deuterium experiment gave split counterpart bands at 1219.9, 1216.7 cm^{-1} and at 1202.4, 1198.6 cm^{-1}, with the latter more photosensitive (Figure 5). We are inclined to assign the upper 1700 and 1234 cm^{-1} bands to GeH_3^- and GeD_3^- and the lower 1670 and 1208 cm^{-1} bands to GeH_2^- and GeD_2^-. This is in accord with observation of only the 1670 cm^{-1} feature at lower H_2 concentration.

Our B3LYP calculation predicts the symmetric Ge−H stretching mode for GeH_3^- slightly higher than the antisymmetric stretching mode, but the BPW91 functional finds the reverse relationship. We believe that the 1700 and 1234 cm^{-1} bands are due to the strong antisymmetric stretching modes of

GeH_3^- and GeD_3^-, and the 1670 and 1208 bands are unresolved stretching modes for GeH_2^- and GeD_2^-. The calculated frequencies are low for both anion species, but they correctly predict the order $GeH_3^- > GeH_2^-$. A similar relationship has been found for $SiH_3^- > SiH_2^-$.[60]

Density functional calculations find the GeH_3^- anion more stable than the GeH_3 radical (35.3 kcal/mol, B3LYP; 34.5 kcal/mol, BPW91), and GeH_2^- more stable than GeH_2 by a lesser amount (21.0 kcal/mol, B3LYP; 22.5 kcal/mol, BPW91), which is consistent with the latter anion being more photosensitive. These are near other theoretical electron affinity values (35.4, 36.8, and 38.0 kcal/mol) and the 37 ± 2 kcal/mol experimental measurement.[57−59] Photodestruction with $\lambda > 380$ nm is overkill, but such is necessary for the matrix-isolated species and lamp sources.[54] Similar studies with SiH_3^- in solid neon find a higher energy $\lambda > 290$ nm requirement for photodestruction of the product absorption.[60]

Reaction Mechanisms. The first reaction observed here is the endothermic (28 kcal/mol)[61] formation of GeH, reaction 1, during deposition with energetic laser-ablated Ge atoms.[62] The exothermic (B3LYP, −25.6 kcal/mol) reaction of Ge atoms with H_2, reaction 2, is expected to be favorable. We note that 8 K annealing increases GeH_2 by 50% (Figure 1), but a similar treatment only sharpens GeD_2 absorptions (Figure 2). Subsequent reactions of GeH_2 with H atoms and molecules, respectively, are also exothermic (B3LYP, −54.6 and −30.1 kcal/mol). Higher level calculations find reaction 4 to be even more exothermic (−36 to −41 kcal/mol).[49] The reaction of GeH with H_2 is also exothermic (B3LYP, −17.2 kcal/mol). However, the observation of GeD and GeD_2 in pure solid deuterium suggests that deuterium reactions may require activation energy, and accordingly, GeD_2 increases on photolysis. In contrast, Si atoms in pure solid deuterium give mostly SiD_4, with no evidence for SiD_2, suggesting that SiD_2 reacts straightaway with D_2 to form SiD_4.[60] It appears that GeH_2 is more reactive than GeD_2: photolysis decreases GeH_2 by 35% and leaves GeD_2 unchanged in solid neon with 5% H_2 and D_2. Finally, recent flash photolysis experiments show that GeH_2 is less reactive than SiH_2.[63]

$$Ge\ (^3P) + H_2\ (^1\Sigma_g^+) \rightarrow GeH\ (^2\Pi) + H\ (^2S) \quad (1)$$

$$Ge\ (^3P) + H_2\ (^1\Sigma_g^+) \rightarrow GeH_2\ (^1A_1) \quad (2)$$

$$GeH_2\ (^1A_1) + H\ (^2S) \rightarrow GeH_3\ (^2A_1) \quad (3)$$

$$GeH_2\ (^1A_1) + H_2\ (^1\Sigma_g^+) \rightarrow GeH_4\ (^1A_1) \quad (4)$$

$$GeH + H_2 \rightarrow GeH_3 \quad (5)$$

$$GeH_3 + GeH_3 \rightarrow Ge_2H_6 \quad (6)$$

$$GeH_2 + GeH_4 \rightarrow Ge_2H_6 \quad (7)$$

The formation of Ge_2H_6 could result from the dimerization reaction 6 of GeH_3 radicals, but the higher absorbance of GeH_2 and GeH_4 suggests that reaction 7 may be more important, as proposed in a photochemical investigation.[64]

Two favorable reactions 8 and 9 contribute to the formation of Ge_2H_2: these are exothermic (B3LYP, −50.5; −53.6 kcal/mol, respectively). Our mixed $H_2 + D_2$ experiment (Figure 4) shows a very weak Ge_2HD absorption between stronger Ge_2H_2 and Ge_2D_2 absorptions, which indicates that reaction 8 contributes most of the Ge_2H_2 observed here. The straightforward formation of Ge_2H_4 involves the dimerization of GeH_2, reaction 10.

$$GeH_2 + Ge \rightarrow Ge_2H_2\ (^1A_1) \quad (8)$$

$$2GeH\ (^2\Pi) \rightarrow Ge_2H_2\ (^1A_1) \quad (9)$$

$$2GeH_2 \rightarrow Ge_2H_4\ (^1A_g) \quad (10)$$

The germyl anion is formed by the capture of ablated electrons during condensation. This electron capture reaction is exothermic by the computed electron affinity (B3LYP, 35.3 kcal/mol) of the GeH_3 radical. The slight growth of GeH_3 radical absorptions on ultraviolet irradiation that destroys GeH_3^- absorptions is probably due to photodetachment of GeH_3^-, the reverse of reaction 11. The GeH_2^- anion formed by electron capture is less stable (electron affinity, B3LYP, 21.0 kcal/mol) and subject to photobleaching at longer wavelengths than GeH_3^-. The reversal in relative yields of GeD_3^- and GeD_2^- from solid neon to solid deuterium follows the increased yield of GeD_3 radical in pure deuterium.

$$GeH_3 + e^- \rightarrow GeH_3^-\ (^1A_1) \quad (11)$$

$$GeH_2 + e^- \rightarrow GeH_2^-\ (^2B_1) \quad (12)$$

Conclusions

Laser-ablated Ge atoms react with H_2 in excess neon and argon during condensation to produce GeH_2 as the major product and GeH, GeH_3, and GeH_4 as minor products. The digermanium Ge_2H_2, Ge_2H_4, and Ge_2H_6 species are also formed. The photosensitive GeH_3^- anion results from the capture of an ablated electron by GeH_3 radical. Identification of these products is based on experiments with different reagent concentrations, HD and D_2 substitution, and agreement with isotopic frequencies from DFT calculations. The novel dibridged Ge_2H_2 species is characterized by a Ge−H_2−Ge stretching mode at 972.2 cm^{-1}, with HD and D_2 counterparts at 934.5 and 715.1 cm^{-1}. The Ge_2H_4 moiety is characterized by a 789.1 cm^{-1} GeH_2 bending mode between values for GeH_4 and Ge_2H_6. The yield of GeH_4 is substantially higher than the yield of GeD_4 in these experiments. All four germanium deuterides are observed in pure deuterium, which shows that further GeD and GeD_2 reactions with D_2 may require activation energy.

Acknowledgment. We gratefully acknowledge support for this work from NSF Grant CHE 00-78836.

References and Notes

(1) Isobe, C.; Cho, H.; Crowell, J. E. *Surf. Sci.* **1993**, *295*, 117.
(2) Lu, G.; Crowell, J. E. *J. Chem. Phys.* **1993**, *98*, 3415.
(3) Simka, H.; Hierlemann, M.; Utz, M.; Jensen, K. F. *J. Electrochem. Soc.* **1996**, *143*, 2646.
(4) Smith, G. R.; Guillory, W. A. *J. Chem. Phys.* **1972**, *56*, 1423.
(5) Lloret, A.; Oria, M.; Seoudi, B.; Abouaf-Marguin, L. *Chem. Phys. Lett.* **1991**, *179*, 329.
(6) Saito, K.; Obi, K. *Chem. Phys. Lett.* **1993**, *215*, 193.
(7) Saito, K.; Obi, K. *Chem. Phys.* **1994**, *187*, 381.
(8) Karolczak, J.; Harper, W. W.; Grev, R. S.; Clouthier, D. J. *J. Chem. Phys.* **1995**, *103*, 2839.
(9) Smith, T. C.; Clouthier, D. J.; Sha, W.; Adam, A. G. *J. Chem. Phys.* **2000**, *113*, 9567.
(10) Becerra, R.; Boganov, S. E.; Egorov, M. P.; Faustov, V. I.; Nefedov, O. M.; Walsh, R. *J. Am. Chem. Soc.* **1998**, *120*, 12657.
(11) Alexander, U. N.; Trout, N. A.; King, K. D.; Lawrance, W. D. *Chem. Phys. Lett.* **1999**, *299*, 291.
(12) Alexander, U. N.; King, K. D.; Lawrance, W. D. *Chem. Phys. Lett.* **2000**, *319*, 529.

(13) Morehouse, R. L.; Christiansen, J. J.; Gordy, W. *J. Chem. Phys.* **1966**, *45*, 1751.
(14) Jackel, G. S.; Christiansen, J.; Gordy, W. *J. Chem. Phys.* **1967**, *47*, 4274.
(15) Kakamura, K.; Takayanagi, T.; Okamoto, M.; Shimokoshi, K.; Sato, S. *Chem. Phys. Lett.* **1989**, *164*, 593.
(16) Johnson, R. D., III; Tsai, B. P.; Hudgens, J. W. *J Chem. Phys.* **1988**, *89*, 4558.
(17) Quandt, R. W.; Hershberger, J. F. *Chem. Phys. Lett.* **1995**, *233*, 559.
(18) Moc, J.; Rudziński, J. M.; Ratajczak, H. *Chem. Phys.* **1992**, *159*, 197.
(19) Bickelhaupt, F. M.; Ziegler, T.; Schleyer, P. v. R. *Organometallics* **1996**, *15*, 1477.
(20) Binning, R. C., Jr.; Curtiss, L. A. *J. Chem. Phys.* **1990**, *92*, 1860.
(21) Das, K.; Balasubramanian, K. *J. Chem. Phys.* **1990**, *93*, 5883.
(22) Huhn, G.; Simon, U.; Petri, M.; Zimmermann, W.; Urban, W. *Mol. Phys.* **1992**, *76*, 1029 and references therein.
(23) Towle, J. P.; Brown, J. M. *Mol. Phys.* **1993**, *78*, 249 and references therein.
(24) Grev, R. S.; DeLeeuw, B. J.; Schaefer, H. F., III. *Chem. Phys. Lett.* **1990**, *165*, 257.
(25) Palágyi, Z.; Schaefer, H. F., III; Kapuy, E. *J. Am. Chem. Soc.* **1993**, *115*, 5, 6901.
(26) Boone, A. J.; Magers, D. H.; Leszczynski, J. *Int. J. Quantum Chem.* **1998**, *70*, 925.
(27) Ricca, A.; Bauschlicher, C. W., Jr. *J. Phys. Chem. A* **1999**, *103*, 11121.
(28) Trinquier, G.; Malrieu, J. P. *J. Am. Chem. Soc.* **1987**, *109*, 5303; *J. Phys. Chem.* **1990**, *94*, 6184. Trinquier, G. *J. Am. Chem. Soc.* **1990**, *112*, 2130.
(29) Liang, C.; Allen, L. C. *J. Am. Chem. Soc.* **1990**, *112*, 1039.
(30) Grev, R. S.; Schaefer, H. F., III; Baines, K. M. *J. Am. Chem. Soc.* **1990**, *112*, 9458.
(31) Jacobsen, H.; Ziegler, T. *J. Am. Chem. Soc.* **1994**, *116*, 3667 and references therein.
(32) Simka, H.; Hierlemann, M.; Utz, M.; Jenson, K. F. *J. Electrochem. Soc.* **1996**, *143*, 2646.
(33) Burkholder, T. R.; Andrews, L. *J. Chem. Phys.* **1991**, *95*, 8697.
(34) Hassanzadeh, P.; Andrews, L. *J. Phys. Chem. A* **1992**, *96*, 9177.
(35) Frisch, M. J.; Trucks, G. W.; Schlegel, H. B.; Scuseria, G. E.; Robb, M. A.; Cheeseman, J. R.; Zakrzewski, V. G.; Montgomery, J. A., Jr.; Stratmann, R. E.; Burant, J. C.; Dapprich, S.; Millam, J. M.; Daniels, A. D.; Kudin, K. N.; Strain, M. C.; Farkas, O.; Tomasi, J.; Barone, V.; Cossi, M.; Cammi, R.; Mennucci, B.; Pomelli, C.; Adamo, C.; Clifford, S.; Ochterski, J.; Petersson, G. A.; Ayala, P. Y.; Cui, Q.; Morokuma, K.; Malick, D. K.; Rabuck, A. D.; Raghavachari, K.; Foresman, J. B.; Cioslowski, J.; Ortiz, J. V.; Stefanov, B. B.; Liu, G.; Liashenko, A.; Piskorz, P.; Komaromi, I.; Gomperts, R.; Martin, R. L.; Fox, D. J.; Keith, T.; Al-Laham, M. A.; Peng, C. Y.; Nanayakkara, A.; Gonzalez, C.; Challacombe, M.; Gill, P. M. W.; Johnson, B. G.; Chen, W.; Wong, M. W.; Andres, J. L.; Head-Gordon, M.; Replogle, E. S.; Pople, J. A. *Gaussian 98*, revision A.7; Gaussian, Inc.: Pittsburgh, PA, 1998.
(36) (a) Becke, A. D. *J. Chem. Phys.* **1993**, *98*, 5648. (b) Lee, C.; Yang, W.; Parr, R. G. *Phys. Rev. B* **1988**, *37*, 785.
(37) (a) Becke, A. D. *Phys. Rev. A* **1988**, *38*, 3098. (b) Perdew, J. P.; Wang, Y. *Phys. Rev. B* **1992**, *45*, 13244.
(38) (a) Krishnan, R.; Binkley, J. S.; Seeger, R.; Pople, J. A. *J. Chem. Phys.* **1980**, *72*, 650. (b) Frisch, M. J.; Pople, J. A.; Binkley, J. S. *J. Chem. Phys.* **1984**, *80*, 3265.
(39) Andrae, D.; Haussermann, U.; Dolg, M.; Stoll, H.; Preuss, H. *Theor. Chim. Acta* **1990**, *77*, 123.
(40) Zhang, L.; Dong, J.; Zhou, M. F. *J. Chem. Phys.* **2000**, *113*, 8700.
(41) Ogden, J. S.; Ricks, M. J. *J. Chem. Phys.* **1970**, *52*, 352.
(42) Hassanzadeh, P.; Andrews, L. *J. Phys. Chem.* **1992**, *96*, 6181.
(43) Gas-phase values are 2114 and 1522 cm^{-1}: Lindeman, L. P.; Wilson, M. K. *J. Chem. Phys.* **1954**, *22*, 1723.
(44) Milligan, D. E.; Jacox, M. E. *J. Chem. Phys.* **1963**, *38*, 2627. Smith, D. W.; Andrews, L. *J. Chem. Phys.* **1974**, *60*, 81.
(45) Crawford, V. A.; Rhee, K. H.; Wilson, M. K. *J. Chem. Phys.* **1962**, *37*, 2377.
(46) Jacox, M. E. *Chem. Phys.* **1994**, *189*, 149.
(47) BelBruno, J. J. *J. Chem. Soc., Faraday Trans.* **1998**, *94*, 1555.
(48) Martin, J. L. M.; Sundermann, A. *J. Chem. Phys.* **2001**, *114*, 3408.
(49) Dyall, K. G. *J. Chem. Phys.* **1992**, *96*, 1210.
(50) Withnall, R.; Andrews, L. *J. Phys. Chem.* **1990**, *94*, 2351.
(51) Lischka, H.; Köhler, H. *J. Am. Chem. Soc.* **1983**, *105*, 6646.
(52) Binkley, J. S. *J. Am. Chem. Soc.* **1984**, *106*, 603.
(53) Goldberg, D. E.; Hitchcock, P. B.; Lappert, M. F.; Thomas, K. M.; Thorne, A. J.; Fjeldberg, T.; Haaland, A.; Schilling, B. E. R. *J. Chem. Soc., Dalton Trans.* **1986**, 2387.
(54) Zhou, M. F.; Andrews, L. *J. Am. Chem. Soc.* **1998**, *120*, 11499.
(55) Zhou, M. F.; Andrews, L. *J. Chem. Phys.* **1999**, *110*, 2414.
(56) Liang, B.; Zhou, M. F.; Andrews, L. *J. Phys. Chem. A* **2000**, *104*, 3905.
(57) Morgon, N. H.; Riveros, J. M. *J. Phys. Chem. A* **1998**, *102*, 10399.
(58) Reed, K. J.; Brauman, J. I. *J. Chem. Phys.* **1974**, *61*, 4830.
(59) Jackson, P.; Sändig, N.; Diefenbach, M.; Schröder, D.; Schwarz, Helmut; Srinivas, R. *Chem. Eur. J.* **2001**, *7*, 151.
(60) Andrews, L.; Wang, X. To be published ($Si + H_2$).
(61) Huber, K. P.; Herzberg, G. *Molecular Spectra and Molecular Structure. IV. Constants of Diatomic Molecules*; Van Nostrand Reinhold: New York, 1979.
(62) Kang, H.; Beauchamp, J. L. *J. Phys. Chem.* **1985**, *89*, 3364.
(63) Becema, R.; Boganov, S. E.; Egorov, M. P.; Nefedov, D. M.; Walsh, R. *Chem. Phys. Lett.* **1996**, *260*, 433.
(64) Piserchio, M. V.; Lampe, F. W. *J. Photochem. Photobiol. A Chem.* **1991**, *60*, 11.